

We are IntechOpen, the world's leading publisher of Open Access books Built by scientists, for scientists

6,900

Open access books available

186,000

International authors and editors

200M

Downloads

Our authors are among the

154

Countries delivered to

TOP 1%

most cited scientists

12.2%

Contributors from top 500 universities



WEB OF SCIENCE™

Selection of our books indexed in the Book Citation Index
in Web of Science™ Core Collection (BKCI)

Interested in publishing with us?
Contact book.department@intechopen.com

Numbers displayed above are based on latest data collected.
For more information visit www.intechopen.com



Cerium Oxide Nanostructures and their Applications

Adnan Younis, Dewei Chu and Sean Li

Additional information is available at the end of the chapter

<http://dx.doi.org/10.5772/65937>

Abstract

Due to excellent physical and chemical properties, cerium oxide (ceria, CeO₂) has attracted much attention in recent years. This chapter aimed at providing some basic and fundamental properties of ceria, the importance of oxygen vacancies in this material, nano-size effects and various synthesis strategies to form diverse structural morphologies. Finally, some key applications of ceria-based nanostructures are reviewed. We conclude this chapter by expressing personal perspective on the probable challenges and developments of the controllable synthesis of CeO₂ nanomaterials for various applications.

Keywords: biofilm, wastewater treatment, biofilm technologies, molecular methods, biofilter media, ceria, metal oxide, nanostructure, nanocomposite, redox reactions, oxygen vacancies

1. Introduction

In nanotechnology, nanomaterials play a vital role in various fields of science, such as physics, chemistry and materials sciences. As a key component of nanomaterials, nanoparticles are single particles or species whose diameter ranges from one to few tens of nanometres. Over the past few years, considerable efforts were made to develop many nanoparticles/nanocrystals for the development of new cutting-edge applications in communications, energy storage, sensing, data storage, optics, transmission, environmental protection, cosmetics, biology and medicine. Due to their limited size and a high density of corner or edge surface sites, the

nanocrystals can exhibit unique physical and chemical properties, including optical, electrical and magnetic properties.

Due to reduced sizes, the nanoparticles possess high surface to volume ratios, which make them highly reactive with distinct characteristics. It is highly desirable to tune the properties of materials through various means such as shapes, morphologies and surface to volume ratios. Over the past few years, the researchers and scientists have made enormous efforts to develop nanoparticles with controlled morphologies, shapes and size. There are various possible synthesis routes, including liquid (chemical method), solid and gaseous media [3–15] for the synthesis of nanocrystals. However, chemical routes are considered as the most popular methods to synthesize nanoparticles, which can offer the advantages of low cost, eco-friendliness and reliability over other methods. Moreover, this method can also offer rigorous control on shape- and size-controlled synthesis of the nanoparticles.

Till now, nanoparticles of many materials, including metal oxides, ferrites, rare-earth oxides and so on, have been developed. Cerium (Ce) belong to rare-earth family and its abundance is much higher than copper and tin (66.5 and 60 ppm, respectively) [1–2]. Its high abundance made this material technologically important with wide applications in various sectors, such as auto-exhaust catalyst [3], low-temperature water-gas shift (WGS) reaction [4], oxygen sensors [5], oxygen permeation membrane systems [6], fuel cells [7, 8], glass-polishing materials [9], electrochromic thin-film application [10], as well as biotechnology, environmental chemistry and medicine [11, 12].

It is generally believed that the reduced particle sizes may originate at high interface densities and hence may lead to enhanced non-stoichiometry levels [13]. Based on this, a lot of attention was paid to explore the nanostructures' ceria interfacial redox reactions and transport properties with respect to bulk ceria.

This chapter is organised as follows. Section 2 presents cerium oxide (CeO_2) and material properties of CeO_2 . Section 3 describes imperfections/defect chemistry in CeO_2 . Section 4 describes the importance of oxygen vacancies in ceria. Section 5 presents nano-size effect. In Section 6, applications of CeO_2 in various fields are described. Finally, Section 7 presents concluding remarks and outlook.

2. Cerium oxide (CeO_2): material properties

2.1. Electronic structure

Cerium dioxide (CeO_2 /ceria) is considered the most stable oxide of the cerium. Cerium is the second member and the most reactive element in the lanthanide series. Being electropositive in nature, cerium exists in dual oxidation modes, Ce^{3+} and Ce^{4+} . The Ce^{4+} oxidation state is usually considered more stable than $3+$ due to $\text{Ce}(4+)$ electronic structure $[\text{Xe}]4f^0$ being more stable state as empty than $[\text{Xe}]4f^1$ for Ce^{3+} . Cerium usually has two types of oxides named cerium dioxide (CeO_2) and cerium sesquioxide (Ce_2O_3), but in a larger context, CeO_2 is used as cerium oxide due to higher stability over Ce_2O_3 .

2.2. Crystal structure

Cerium dioxide (CeO_2) has a fluorite structure (FCC) with space group $\text{Fm}\bar{3}\text{m}$ and it consists of a simple cubic oxygen sub-lattice with the cerium ions occupying alternate cube centres as shown in **Figure 1**. **Figure 1** illustrates the structure of the stoichiometric CeO_2 with the four coordinated oxygen (represented by solid red big balls) and the eight coordinated cerium (represented by solid blue small balls). Cerium is at the centre of tetrahedron whose corners are occupied by oxygen atoms [14].

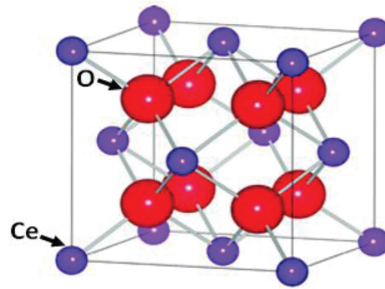


Figure 1. FCC structure for CeO_2 [14].

2.3. Microstructure

The microstructure of CeO_2 thin films can be of various shapes depending on substrate material, deposition method, deposition parameters and composition contents. Therefore, the film growth can result in epitaxial films on the one hand or polycrystalline films with varying grain sizes from few nanometres up to several hundred micrometres on the other hand. Polycrystalline films consist of a certain number of grains, which can play a key role in the electrical conduction process in thin films by forming depletion layers with low conductivity similar to Schottky barriers in metal-insulator junctions [15].

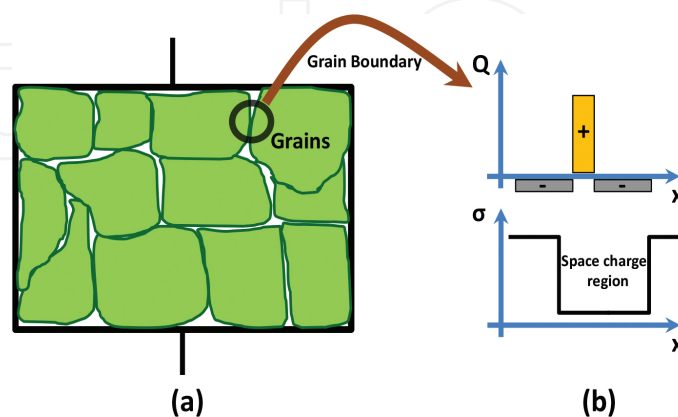


Figure 2. (a) Cross-section of a polycrystalline thin film capacitor showing grains. The crystal orientation and size of the grains depends on the preparation parameters. (b) Space charge region and the consequent change of the conductivity at the grain boundaries.

Figure 2(a) represents a schematic cross-section of a ceramic thin film capacitor with grains randomly distributed in between capacitor plates. The region between the grains in **Figure 2(b)** shows the space-charge region and the reduced conductivity due to the immovable positive charges. For thin films with smaller grain sizes, the space-charge region can exceed the grain size, leading to entirely depleted films with locally distributed conductivities far below the bulk conductivity of the material [16].

3. Imperfections/defect chemistry in bulk ceria

For an ideal crystalline solid, atoms are periodically arranged in a regular and symmetrical way. The formation of a crystal structure is based on the combination of a basis and infinite space lattice. This space lattice can be further split into unit cells and the combination of identical cells forms the entire crystalline structure. Imperfections in crystal structures are occurred by displacing atoms from their lattice positions that lead to break symmetry of the perfect periodic crystal lattice. In ceria, the intrinsic and extrinsic defects can exist. The presence of intrinsic defect may be due to thermal disorderness in crystal, which can be formed by redox reactions between the solid and surrounding atmosphere. Frenkel and Schottky defects are considered to be more plausible crystalline intrinsic defects. The extrinsic defects in crystal may be formed by introducing foreign dopant or due to impurities.

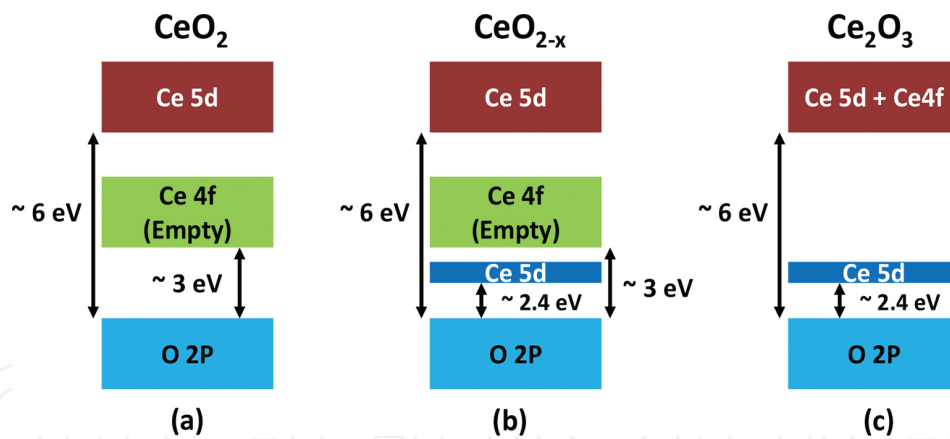


Figure 3. Schematic electronic structures of (a) stoichiometric CeO_2 , (b) partially reduced CeO_{2-x} and (c) Ce_2O_3 . Blue blocks represent filled bands, whereas green and red blocks are drawn as empty boxes.

The most dominant and stable known defects in ceria are linked to the presence of oxygen vacancies under a wide range of conditions. A reversible transition in the oxidation state of two cerium ions from Ce^{3+} to Ce^{4+} may generate neutral oxygen vacancies in ceria. The process can be shown as



Thus, a neutral species $\frac{1}{2}\text{O}_2(\text{g})$ is formed if an oxygen ion (O^{2-}) leaves the ceria lattice. The two electrons left behind were trapped at two cerium sites, i.e. they become localized at two cerium sites. At such cerium sites, the electron prefers to occupy an empty Ce4f state that splits the Ce4f band into two sub-bands: an occupied Ce4f full band and an empty Ce4f empty band as shown in **Figure 3**.

Practically, the reduction limit of non-stoichiometric ceria is Ce_2O_3 , where all cerium ions are found in a Ce^{3+} oxidation state. The electronic band structure of Ce_2O_3 bears resemblance to that of partially reduced ceria, in which Ce4f empty and Ce5d bands have been merged together in the conduction band as shown in **Figure 3(c)**.

4. Importance of oxygen vacancies in CeO_2

Cerium oxide can accommodate high oxygen deficiency by the substitution of lower valent elements on the cation sub-lattice. Due to this property, high oxygen ion conductivities are expected, which indicate towards its potential applications as a solid electrolyte in solid oxide fuel cells (SOFCs) [17]. At the same time, CeO_2 is also well known to release significant levels of oxygen at low oxygen partial pressures (P_{O_2}) and elevated temperatures leading to a mixed ionic electronic conductivity. Due to ease in redox-based reactions, ceria can easily occupy multiple oxidation states such as $\text{Ce}(3+)$ and $\text{Ce}(4+)$; therefore, electrons in ceria can be thought to exist as small polarons. The motion of the electrons in the ceria lattice can be imagined as a thermally mediated hopping mechanism [18]. For carrier and transport properties, the concentration of vacancies that are more mobile and can contribute to oxygen-ion transport in the solid solutions should be taken into account [19].

Generally, three low-index lattice planes exist on the surface of CeO_2 nanocrystals: (100), (110) and (111). From **Figure 4**, the stability of all three planes is different and follows the sequence $(111) > (110) > (100)$, whereas the activity follows the reverse order [20–23].

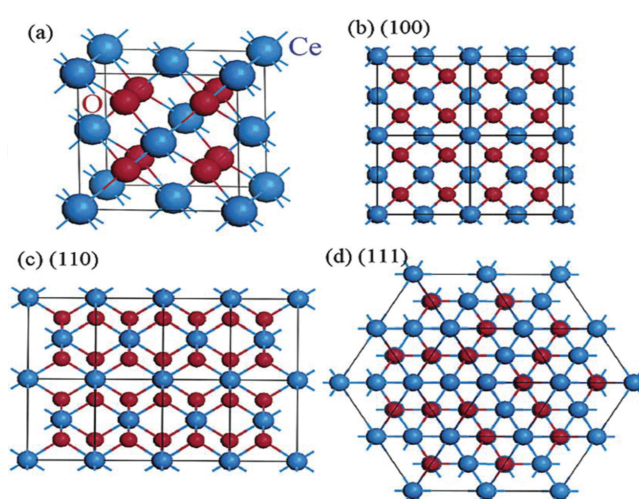


Figure 4. (a) Face-centred crystal cell of the CeO_2 structure. (b–d) The (100) [or (200)], (110) and (111) planes of the CeO_2 structure. (Reprinted with permission from reference [24] © 2003 American Chemical Society.)

The formation energy of oxygen vacancies at (111) exposed facet is higher than (110) and (100) facets; therefore, there are more oxygen vacancies on the (110) and (100) planes than (111). For example, nanoparticles usually constitute octahedral or truncated octahedral shapes and they are mainly exposed to most stable (111) facets to keep surface energy as minimum as possible. While 1D nanostructures such as nanorods and nanowires possess the (110) and (100) planes, 3D nanocubes can expose (100) planes. Therefore, nanorods and nanocubes should have more oxygen vacancies on their surfaces. Meanwhile, the concentration of oxygen vacancies in the crystal can also be influenced by many other internal or external factors, such as temperature and doping elements, etc. [25]. The existence of oxygen vacancies and their transportation in crystal are very important phenomena. Higher concentration of oxygen vacancies provides ease in the movement of oxygen atoms within crystal, which favour redox reactions on its surface for excellent catalytic activities.

5. Nano-size effects

By decreasing particle size, ceria nanoparticles demonstrate the formation of more oxygen vacancies. The large surface area to volume ratio existing in a nanoparticle enables CeO_2 to react differently resulting in unique properties. For instance, two orders of magnitude high catalytic activity for CO oxidation was observed by synthesizing 3–4 nm sized CeO_2 nanoparticles supporting Au over a regular bulk cerium oxide support medium [26, 31]. Therefore, it is feasible to tune the specific reactivity of ceria nanoparticles by controlling their size. Furthermore, nano-sized CeO_2 can have enhanced electronic conductivity, size lattice relaxation and many other effects as compared to bulk ceria.

Additionally, for determining particle reactivity, building nano-sized particle is very crucial in a way that the lattice of nanoceria expands if the particle size is reduced. The expansion of lattice would decrease its oxygen release and reabsorption capabilities. A detailed electron diffraction study on nanoceria was conducted previously [27] in which a systematic lattice expansion was observed by reducing the size of ceria particles down to nanoscale over bulk ceria. Their findings suggested that by having ultra-small-sized (1.1 nm) ceria nanoparticle, a large fraction of the cerium atoms occupy fully reduced state, even though the ceria nanoparticles retain a cubic-shaped lattice rather than hexagonal lattice [27]. In another theoretical study on ceria nanoparticles, the simulation calculations revealed that by increasing ceria particle size the formation energy of oxygen vacancies is reduced [28].

6. Applications of ceria

Being technologically important functional material, ceria has remarkable applications in many diverse fields. In this section, a brief discussion on some of the most widely known commercial and industrial applications of ceria and nanoceria is presented.

6.1. Solid oxide fuel cells

Solid oxide fuel cells (SOFCs) are considered to have great potential in providing clean and reliable electric power; therefore, research in this area attracts great attention in recent years. Many reports suggest that ceria-based ion conductors possess huge resistance to carbon deposition and have potential to allow unstoppable supply of dry hydrocarbon fuels to the anode [29, 30].

Gorte and Vohs [31] first demonstrated a direct electrochemical oxidation of hydrocarbons such as methane and toluene using SOFC at 973 and 1073 K with copper and ceria composite. The anode was designed as Cu/CeO₂/YSZ, with Cu primarily utilized as the current collector and the function of CeO₂ was to impart catalytic activity for the required oxidation reactions. These anodes were found to have inherently high redox stability, large sulphur tolerance and were operative with sulphur contents up to 400 ppm without losing its significance performance [32].

Ceria-based ceramics are well known to exhibit mixed ionic and electronic conductivity in a reducing atmosphere due to reversible redox transition between Ce³⁺ and Ce⁴⁺. Additionally, their excellent catalytic activities also correspond to ease in an oxygen-vacancy formation mechanism. Another effective method to increase the reforming reactions of hydrocarbon, i.e. to facilitate C–H bond breaking process is the addition of noble metals, such as Pt, Rh, Pd and Ru.

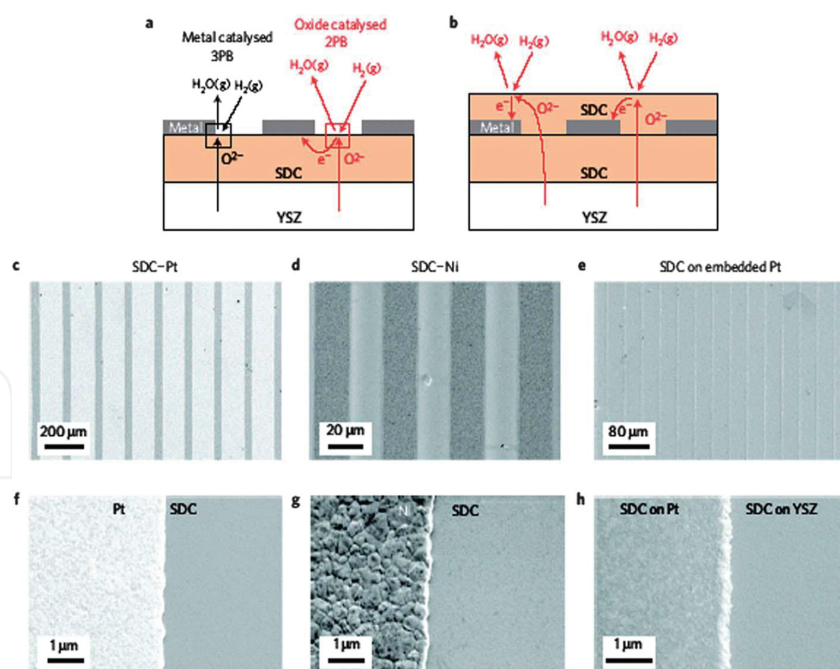


Figure 5. Metal patterning on ceria thin films. (a) Schematic figure showing the macroscopic reaction sites and the steps involved for surface reaction and bulk diffusion. (b) Patterned electrode with an embedded current collector that restricts the metallic phase contribution. (c–h) After electrochemical characterisation, the SEM images were recorded under humid atmospheres at 650C. (SDC $\frac{1}{4}$ Sm_{0.2}Ce_{0.8}O_{1.9}d, YSZ $\frac{1}{4}$ Y_{0.16}Zr_{0.84}O_{1.92}). (Reprinted from reference [35] with permission from Nature Publishing Group.)

Gd-doped CeO₂-based electrolyte films having Ru and Ni as incorporated metals were fabricated to evaluate the role of metal catalysts in anode reactions by Hibino et al. [33, 34].

The anodes were directly operated on various hydrocarbons at 600°C and the results demonstrated that the presence of Ru catalyst favours the reforming reactions of unreacted hydrocarbons by steam and carbon dioxide. This further avoids the gas-phase diffusion of fuels by restricting the interference of steam and CO₂. The obtained power density in this case was 750 mW cm⁻² with dry methane, which was quite analogous to the power density of 769 mW cm⁻² achieved with wet hydrogen [33, 34].

The reduction of activation over potential for hydrogen oxidation by having ceria-based anodes for SOFC has been exemplified in many reports. Moreover, well-defined geometry and having porous or composite electrodes structure based on ceria were also described. In a report, Chueh et al. [35] demonstrated well-defined interferences occupied ceria-metal structures, in which near-equilibrium H₂ oxidation reaction pathway was subjugated by electrocatalysis at the oxide-gas interface with a minimal contribution that was observed from oxide-metal-gas triple-phase boundaries as shown in **Figure 5**. The similar phenomenon was observed even for structures with reaction site densities approaching those of commercial SOFCs [35].

By keeping the ceria-catalysed reaction site density fixed as 2PB, the density of metal-catalysed reaction site (3PB) was varied by a factor of 16; no substantial change was observed in the electrochemical activity. Later on, the addition of metals did not put much impact on the electrochemical activities, respectively. They conclude that the rational design of ceria nanostructures promote electrochemical activities and thus provide a new route to achieve high performance [35].

6.2. Catalytic applications

The tendency of oxygen uptake and release of ceria due to reversible transition between Ce³⁺ and Ce⁴⁺ makes this material a key ingredient for catalytic applications and reactions. Various nano-micro ceria structures have been fabricated, and their catalytic applications are extensively reported in recent years.

Carbon monoxide (CO) oxidation is the most exclusively studied reaction in this category. During CO oxidation, ceria nanomaterials can elevate the oxygen storage capability of catalysts at low temperatures. Generally, high surface area occupied nanomaterials are considered ideal for this application. The high surface area provides a greater tendency to active species to contact with reactants, and therefore an enhanced catalytic performance can be expected. There are different reports that discuss various morphologies to evaluate the CO oxidation performance. For instance, nanotubes exhibit inner and outer surfaces that unadventurously provide active sites for the reactants adsorption that leads to better catalytic performance in CO oxidation [36]. On the other hand, nano-sized particles also exhibit high surface area, but demonstrate poor catalytic performance; while nanorods, with low surface area and larger diameter, were found to be more active in CO oxidation [37–40]. This unusual behaviour of diverse morphologies is mainly attributed to the exposed planes. For example, the nanoparticles have dominant (111) exposed planes, whereas the nanorods' edges are terminated by

(110) and (100) planes. The (110) and (100) planes are considered to be more active than the (111) plane and hence are found to express significantly enhanced redox properties required for excellent catalytic activities in CO oxidation.

In a study, Kayama et al. [41] introduced a new concept of fabricating ceria particles' aggregates around central silver metal (rice-ball-like structure) which is quite different than conventional core-shell-like configuration. The catalytic activities of fabricated structure were evaluated, and it was found that below 300°C CeO₂-Ag oxidizes soot much more efficiently than pure CeO₂ and Ag-CeO₂ that oxidize soot above 300°C as shown in **Figure 6**.

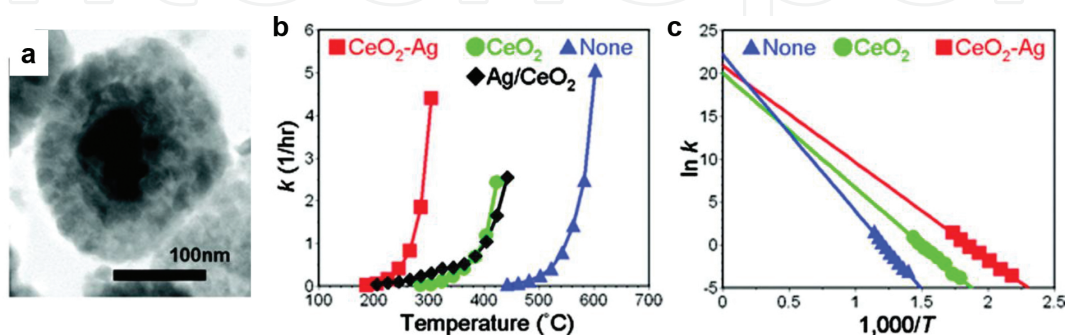


Figure 6. (a) Transmission electron microscopy image of rice-ball nanostructured CeO₂-Ag; (b and c) evaluation of properties in the presence and absence of a catalyst; (b) evaluations of carbonaceous soot oxidation; (c) Arrhenius plots. (Reprinted with permission from reference [41]. Copyright 2010 American Chemical Society.)

In the absence of rice-ball nanostructure, the oxidation by the catalyst was inefficient at low temperatures below 300°C. Therefore, it was suggested that the synthesis mechanism of the rice-ball-like structure can potentially be extended to other compositions.

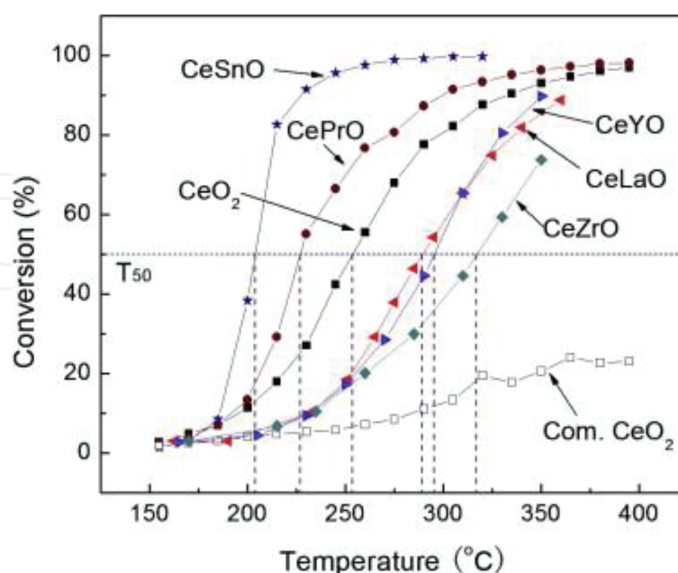


Figure 7. Conversion profile of carbon monoxide versus temperature. (Reprinted from reference [42] with permission from Elsevier Ltd.)

Doping foreign elements into ceria matrix can considerably tune the inherent physical and chemical properties of ceria. To keep this in mind, Y-, La-, Zr-, Pr- and Sn-doped ceria were reported by Xiao et al. [42]. In their work, they fabricated a flower-like structure, and the catalytic activities towards CO oxidation were recorded for all dopant elements as shown in **Figure 7**.

From the figure, two main observations were recorded. (i) The doping of Sn and Pr enhanced the catalytic activities of ceria-based nanoflower structure and this behaviour was attributed to the variable valence states of Pr and Sn. (ii) The doping of Y, La and Zr in CeO₂ did not express considerable catalytic activities, and this trend was explained on the basis of the stable valence states of dopants. Also, they suggested that the doping cations having stable valence state partially suppress the redox reactions, i.e. Ce⁴⁺ to Ce³⁺ conversion which ultimately suppress the oxygen storage capacity in ceria.

6.3. Photocatalysis

Globally, efficient visible light photocatalytic water splitting is an active area of research for renewable energy as well as water and air purification. A novel and efficient Au-supported CeO₂ nanoparticle-based photocatalysts were fabricated, and its visible light activities were reported by Primo et al. [43]. Excellent photocatalytic activity of ceria nanoparticles was observed for oxygen generation from water as shown in **Figure 8**.

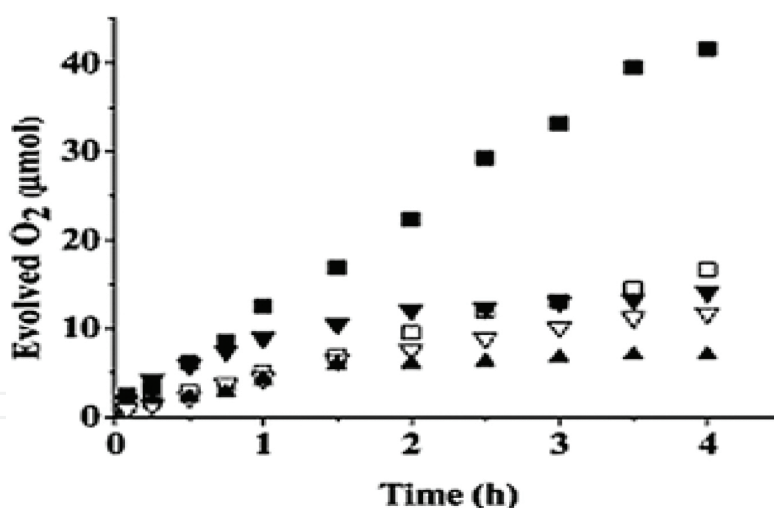


Figure 8. (a) Oxygen evolved upon visible light ($\lambda > 400$ nm) illumination of an aqueous AgNO₃ suspension containing the photocatalysts. ■ Au (1.0 wt%)/CeO₂ (A); □ Au (1.0 wt%)/CeO₂ (B); ▼ Au (3.0 wt%)/CeO₂ (A); ▽ Au (3.0 wt%)/CeO₂ (B); ▲ WO₃.CeO₂ (A) was prepared by biopolymer template synthesis whilst CeO₂ (B) was obtained from Aldrich. (Reprinted with permission from reference [43]. Copyright 2011 American Chemical Society.)

Figure 8 shows the evolved oxygen over time for visible-light illumination for various Au loadings on CeO₂ catalysts. The sample, with 1.0 wt% loading of Au, renders a more profound photocatalyst than 3.0 wt% Au. Under UV light illumination, the ceria sample (A) prepared by the novel biopolymer template procedure having smaller particle size was found to be more efficient than the large particle-sized occupied commercial CeO₂ (B) sample. Their observations

were quite different from other reports on TiO_2 and WO_3 , in which under UV light, the photocatalytic activity was poor and reduced, while Au-supported CeO_2 delivers outclass photocatalytic response under visible light.

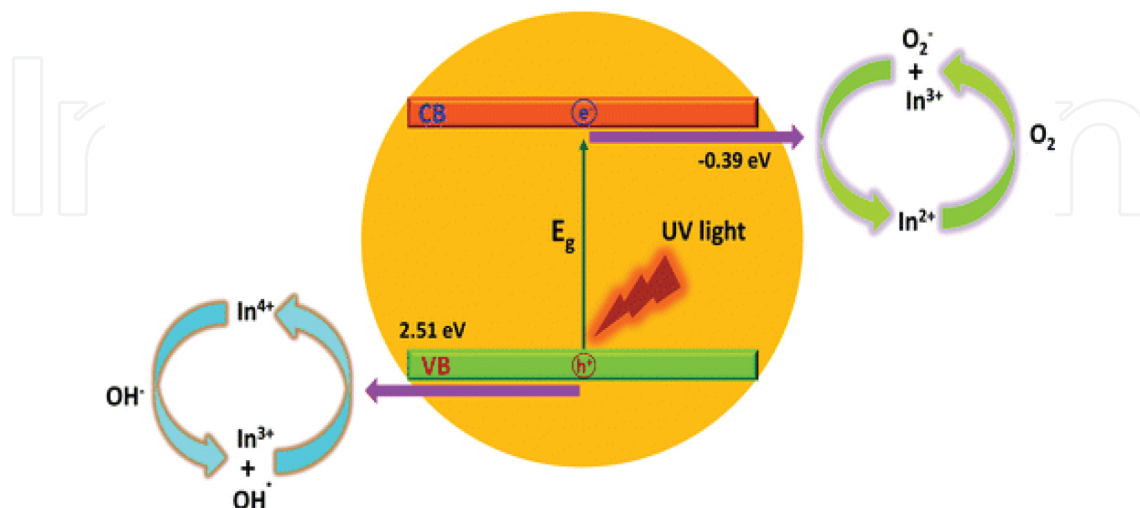


Figure 9. Schematic diagram of the degradation mechanisms for the MO dye with indium doped CeO_2 nanocrystals under ultraviolet-visible light irradiation. (Reprinted with permission from reference [44].)

Recently, our group has successfully synthesized ultra-small-sized ceria nanocubes. The effect of indium doping on oxygen vacancies' concentration and subsequently on photocatalytic response was investigated in detail [44]. Various In doping concentrations ranging from 0, 5 to 15% were fabricated and their photocatalytic responses were evaluated. By increasing Indium doping concentration, the photocatalytic activities were found to be enhanced up to a certain extent (10% In doping). After this doping concentration, the photocatalytic activities were suppressed. The possible reason may be due to the presence of In^{3+} , which may serve as an electron acceptor and electron donor simultaneously (from In^{3+} to In^{2+} and/or from In^{3+} to In^{4+}) to localize the charge carriers. This localization may further enlarge the separation of electron-hole pairs by trapping at energy levels in close proximity to the valence and conduction bands [44]. This effect is schematically described in **Figure 9**.

Ceria nanomaterials have also a potential application for environmental remediation. The photocatalytic activities of CeO_2 nanotubes and nanoparticles were investigated and compared with commercial TiO_2 (P25) as shown in **Figure 10** [45]. A well-known toxic pollutant named 'aromatic benzene' that is commonly found in urban ambient air and is of substantial concern regarding environmental health was used in photocatalytic measurements.

The results in **Figure 10** demonstrate that at the reaction time of 22 h, the CeO_2 -NT expressed excellent photocatalytic performance towards the gas-phase degradation of benzene. The amount of CO_2 over CeO_2 -NT was maintained at 29 ppm even after 10 h of reaction time. On the contrary, ceria nanoparticles and P25 nanoparticles demonstrate quite uneven photocatalytic behaviour of benzene degradation.

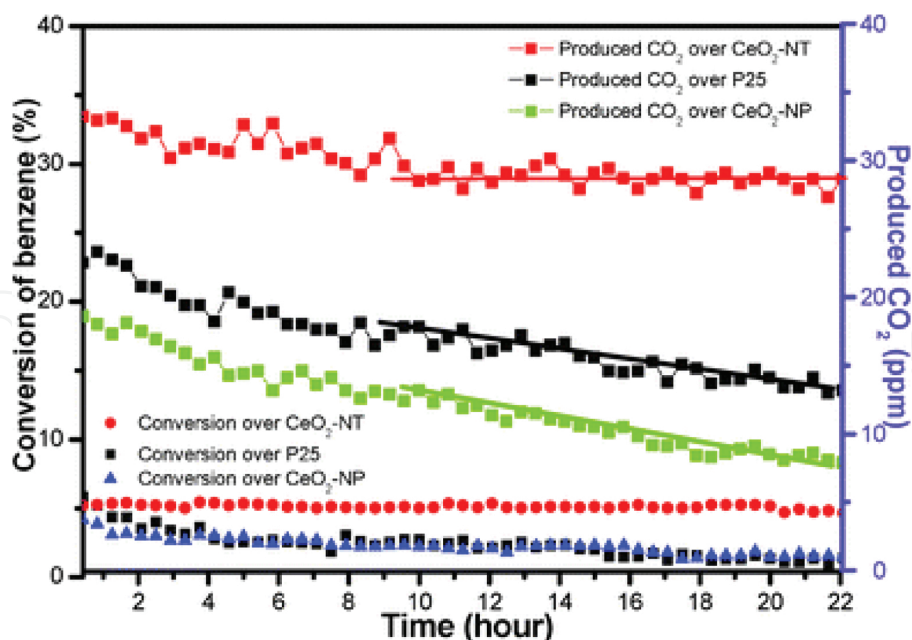


Figure 10. Time-online data for gas-phase photocatalytic degradation of benzene over the samples of commercial P25, CeO₂ nanoparticles (NPs) and the as-prepared CeO₂ nanotubes (NTs). (Reprinted from reference [45] with permission from Royal Society of Chemistry.)

7. Concluding remarks and future outlook

In this chapter, some fundamental physical and chemical properties of ceria were addressed in the beginning. In the later half, recent progress in the shape-controlled synthesis and morphology-dependant performance of ceria nano-microstructures was highlighted. Although, the microstructures, morphologies, characterization approaches and theoretical studies of ceria-based nanostructured materials are extensively investigated in recent years with the achievement of some exceptional encouraged results. However, there are still numerous contests such as cost-effective synthetic processes for morphology-dependent catalytic and biomedical applications that required more efforts to tackle the key fundamental issues.

Another important fatal issue in the preparation of ceria-based materials is 'Sintering'. Particles can easily agglomerate at high temperatures, which is a big reason for sudden drop in specific surface area of nanomaterials and reduced crystal defects. Although, the addition of rare-earth elements somehow facilitates anti-sintering phenomenon; however, this restricts the limitation of special additives in ceria-based nanomaterials. Therefore, to spread the span of nanoceria applications, this problem needs to be addressed comprehensively. Finally, vast scale production of ceria nanomaterials is also challenging. It is essentially required to develop and improve more valuable preparation of technologies for industrial and commercial applications combined with deepening comprehension of the formation mechanisms.

Author details

Adnan Younis*, Dewei Chu and Sean Li

*Address all correspondence to: a.younis@unsw.edu.au

School of Materials Science and Engineering, University of New South Wales, Sydney, Australia

References

- [1] Ahrens TJ. *Global Earth Physics: Handbook of Physical Constants*, American Geophysical Union, Washington DC. 1995.
- [2] Lide D. *CRC Handbook of Chemistry and Physics*, CRC Publishing Co., Boca Raton, FL. 88th edn. 2007.
- [3] Kaspar J, Fornasiero P, Graziani M. Use of CeO₂-based oxides in the three-way catalysis. *Catalysis Today*. 1999; 50(2): 285–298.
- [4] Fu Q, Saltsburg H, Flytzani-Stephanopoulo M. Active nonmetallic Au and Pt species on ceria-based water–gas shift catalysts. *Science*. 2003; 301(5635): 935–938.
- [5] Jasinski P, Suzuki T, Anderson HU. Nanocrystalline undoped ceria oxygen sensor. *Sensors and Actuators B Chemical*. 2003; 95(1):73–77
- [6] Yin X, Hong L, Liu ZL. Oxygen permeation through the LSCO-80/CeO₂ asymmetric tubular membrane reactor. *Journal of Membrane Science*. 2006;268(1): 2–12.
- [7] Park SD, Vohs JM, Gorte RJ. Direct oxidation of hydrocarbons in a solid oxide fuel cells. *Nature*. 2000; 404: 265–267.
- [8] Sun CW, Hui R, Roller J. Cathode materials for solid oxide fuel cells: a review. *Journal of Solid State Electrochemistry*. 2010; 14(7):1125–1144.
- [9] Feng XD, Sayle DC, Wang ZL, Paras MS, Santora B, Sutorik AC, Sayle TXT, Yang Y, Ding Y, Wang XD, Her YS. Converting ceria polyhedral nanoparticles into single-crystal nanospheres. *Science*. 2006; 312(5779):1504–1508.
- [10] Ozer N. Optical properties and electrochromic characterization of sol–gel deposited ceria films. *Solar Energy Materials and Solar Cells*. 2001; 68(3–4): 391–400.
- [11] Asati A, Santra S, Kaittanis C, Nath S, Perez JM. Oxidase-like activity of polymer-coated cerium oxide nanoparticles. *Angewandte Chemie International Edition*. 2009; 48: 2308–2312. doi:10.1002/anie.200805279.

- [12] Tarnuzzer RW, Colon J, Patil S, Seal S. Vacancy engineered ceria nanostructures for protection from radiation-induced cellular damage. *Nano Letters*. 2005; 5: 2573–2577.
- [13] Tuller HL, Ionic conduction in nanocrystalline materials. *Solid State Ionics*. 2000; 131: 143–157.
- [14] Malavasi L, Fisher CAJ, Islam MS. Oxide-ion and proton conducting electrolyte materials for clean energy applications: structural and mechanistic features. *Chemical Society Reviews*. 2010; 39(11): 4370–4387.
- [15] Neumann H, Arlt G. Maxwell-Wagner relaxation and degradation of SrTiO₃ and BaTiO₃ ceramics. *Ferroelectrics*. 1986; 69(1): 179–186.
- [16] Waser R. The role of grain boundaries in conduction and breakdown of perovskite-type titanates. *Ferroelectrics*. 1992; 133(1): 109–114.
- [17] Guo X, Waser R. Electrical properties of the grain boundaries of oxygen ion conductors: acceptor-doped zirconia and ceria. *Progress in Materials Science*. 2006; 51: 151–210.
- [18] Tuller HL, Nowick AS. Small polaron electron-transport in reduced CeO₂ single-crystals. *Journal of Physics and Chemistry of Solids*. 1977; 38: 859–867.
- [19] Kilner JA. Defects and conductivity in ceria-based oxides. *Chemical Letters*. 2008; 37: 1012–1015.
- [20] Sayle DC, Maicaneanu SA, Watson GW. Atomistic models for CeO₂(111), (110), and (100) nanoparticles, supported on yttrium-stabilized zirconia. *Journal of American Chemical Society*. 2002; 124(138): 11429–11439.
- [21] Jiang Y, Adams JB, van Schilfhaarde M. Density-functional calculation of CeO₂ surfaces and prediction of effects of oxygen partial pressure and temperature on stabilities. *Journal of Chemical Physics*. 2005; 123: 064701.
- [22] Chen Y, Hu P, Lee MH, Wang H. Au on (1 1 1) and (1 1 0) surfaces of CeO₂: a density-functional theory study. *Surface Science*. 2008; 602(10): 1736–1741.
- [23] Sayle TXT, Cantoni M, Bhatta UM, Parker SC, Hall SR, Möbus G, Molinari M, Reid D, Seal S, Sayle DC. Strain and architecture-tuned reactivity in ceria nanostructures; enhanced catalytic oxidation of CO to CO₂. *Chemistry of Materials*. 2012; 24(10): 1811–1821.
- [24] Wang ZL, Feng XD. Polyhedral shapes of CeO₂ nanoparticles. *Journal of Physical Chemistry B*. 2003; 107: 13563–13566.
- [25] Campbell CT, Peden CHF. Oxygen vacancies and catalysis on ceria surfaces. *Science*. 2005; 309: 713–714
- [26] Carrettin S, Concepcion P, Corma A, Nieto JML, Puntès VF. Nanocrystalline CeO₂ increases the activity of Au for CO oxidation by two orders of magnitude. *Angewandte Chemie International Edition*. 2004; 43: 2538–2540.

- [27] Hailstone RK, DiFrancesco AG, Leong JG, Allston TD, Reed K. J. A study of lattice expansion in CeO₂ nanoparticles by transmission electron microscopy. *Journal of Physical Chemistry C*. 2009; 113(34): 15155–15159
- [28] Migani A, Vayssilov GN, Bromley ST, Illas F, Neyman KM. Dramatic reduction of the oxygen vacancy formation energy in ceria particles: a possible key to their remarkable reactivity at the nanoscale. *Journal of Material Chemistry*. 2010; 20: 10535–10546.
- [29] Marina OA, Mogensen M. High-temperature conversion of methane on a composite gadolinia-doped ceria–gold electrode. *Applied Catalysis A*. 1999; 189: 117–126.
- [30] Gorte RJ, Vohs JM. Nanostructured anodes for solid oxide fuel cells. *Current Opinion on Colloid and Interface Science*. 2009; 14: 236–244.
- [31] Park SD, Vohs JM, Gorte RJ. Direct oxidation of hydrocarbons in a solid oxide fuel cells. *Nature*. 2000; 404: 265–267.
- [32] He HP, Gorte RJ, Vohs JM. Highly sulfur tolerant Cu–ceria anodes for SOFCs. *Electrochem. Solid-State Letters*. 2005; 8: A279–A280.
- [33] Hibino T, Hashimoto A, Yano M, Suzuki M, Sano M. Ru-catalyzed anode materials for direct hydrocarbon SOFCs. *Electrochimica Acta*. 2003; 48:2531–2537.
- [34] Hibino T, Hashimoto A, Asano K, Yano M, Suzuki M, Sano M. An intermediate-temperature solid oxide fuel cell providing higher performance with hydrocarbons than with hydrogen. *Electrochemical and Solid-State Letters*. 2002; 5:A242–A244.
- [35] Chueh WC, Hao Y, Jung W, Haile SM. High electrochemical activity of the oxide phase in model ceria–Pt and ceria–Ni composite anodes. *Nature Materials*. 2012; 11: 156–161.
- [36] Pan CS, Zhang DS, Shi LY. CTAB assisted hydrothermal synthesis, controlled conversion and CO oxidation properties of CeO₂ nanoplates, nanotubes, and nanorods. *Journal of Solid State Chemistry*. 2008; 181: 1298–1306.
- [37] Tana, Zhang M, Li J, Li H, Li Y, Shen W. Morphology-dependent redox and catalytic properties of CeO₂ nanostructures: nanowires, nanorods and nanoparticles. *Catalysis Today*. 2009; 148: 179–183,
- [38] Zhang DS, Niu FH, Yan TT, Shi LY, Du XJ, Fang JH. Ceria nanospindles: template-free solvothermal synthesis and shape-dependent catalytic activity. *Applied Surface Science*. 2011; 257: 10161–10167.
- [39] Pan CS, Zhang DS, Shi LY, Fang JH. Template-free synthesis, controlled conversion, and CO oxidation properties of CeO₂ nanorods, nanotubes, nanowires, and nanocubes. *European Journal of Inorganic Chemistry*. 2008; 2008(15): 2429–2436.
- [40] Wu Z, Li M, Overbury SH. On the structure dependence of CO oxidation over CeO₂ nanocrystals with well-defined surface planes. *Journal of Catalysis*. 2012; 285: 61–73.

- [41] Kayama T, Yamazaki K, Shinjoh H. Nanostructured ceria–silver synthesized in one-pot redox reaction catalyzes carbon oxidation. *Journal of American Chemical Society*. 2010; 132: 13154–13155.
- [42] Xiao GL, Li S, Li H, Chen LQ. Synthesis of doped ceria with mesoporous flower-like morphology and its catalytic performance for CO oxidation. *Microporous and Mesoporous Materials*. 2009; 120: 426–431.
- [43] Primo A, Marino T, Corma A, Molinari R, García H. Efficient visible-light photocatalytic water splitting by minute amounts of gold supported on nanoparticulate CeO₂ obtained by a biopolymer templating method. *Journal of American Chemical Society*. 2011; 133: 6930–6933.
- [44] Younis A, Chu D, Kaneti YV, Li S. Tuning the surface oxygen concentration of {111} surrounded ceria nanocrystals for enhanced photocatalytic activities. *Nanoscale*. 2016; 8(1): 378–387.
- [45] Tang Z, Zhang Y, Xu Y. A facile and high-yield approach to synthesize one-dimensional CeO₂ nanotubes with well-shaped hollow interior as a photocatalyst for degradation of toxic pollutants. *RSC Advances*. 2011; 1: 1772–1777.